

# Rare decay $B \rightarrow X_s \nu \bar{\nu}$ in the two-Higgs-doublet model of type-III

Zhenjun Xiao<sup>1\*</sup>, Liping Yao<sup>2</sup>

<sup>1</sup> Department of Physics, Nanjing Normal University, Nanjing, Jiangsu 210097, P.R.China

<sup>2</sup> Department of Physics, Henan Normal University, Xinxiang, Henan 453002, P.R.China

(October 28, 2018)

## Abstract

In this paper, we calculated the new physics contribution to theoretically very clean rare decay  $B \rightarrow X_s \nu \bar{\nu}$  in the general two-Higgs-doublet model (model III). Within the considered parameter space, we found that (a) the new physics contribution can provide one to two orders of enhancement to the branching ratio  $\mathcal{B}(B \rightarrow X_s \nu \bar{\nu})$  and can saturate the experimental bound on  $\mathcal{B}(B \rightarrow X_s \nu \bar{\nu})$  in some regions of the parameter space; (b) besides the CLEO data of  $B \rightarrow X_s \gamma$ , the ALEPH upper limit on  $\mathcal{B}(B \rightarrow X_s \nu \bar{\nu})$  also lead to further constraint on the size of the Yukawa coupling  $\lambda_{tt}$ :  $\lambda_{tt} < 6.4$  for  $\lambda_{bb} = 2.7$  and  $m_{H^+} = 200$  GeV.

PACS: 12.60.Fr, 13.20.He, 13.40.Ks, 12.15.Ji,

Key words: Rare B meson decays, Two-Higgs-Doublet model, Yukawa coupling

---

\*Email address: zjxiao@email.njnu.edu.cn

In the standard model (SM), the rare decays  $B \rightarrow X_{s,d} \nu \bar{\nu}$  are fully dominated by the  $Z^0$ -penguin and box diagrams involving top quark exchanges. The charm quark contribution and the long distance contributions are negligible, and the theoretical uncertainties related the renormalization scale dependence of running quark mass can be essentially neglected after the inclusion of next-to-leading order corrections [1]. These decays are theoretically very clean processes in the field of rare B-decays and are also sensitive to the new physics beyond the SM [2,3,4].

The decays  $B \rightarrow X_{s,d} \nu \bar{\nu}$  have been thoroughly studied in [3] and reviewed recently in [1]. Normalizing to the semi-leptonic branching ratio  $\mathcal{B}(B \rightarrow X_c e \bar{\nu})$  and summing over the three neutrino flavors, one finds [1]

$$\mathcal{B}(B \rightarrow X_q \nu \bar{\nu}) = \mathcal{B}(B \rightarrow X_c e \bar{\nu}) \frac{3\alpha_{em}^2}{4\pi^2 \sin^4 \theta_W} \frac{|V_{tq}|^2}{|V_{cb}|^2} \frac{|X(x_t)|^2}{f(z)} \frac{\bar{\eta}}{\kappa(z)} \quad (1)$$

where  $q = (d, s)$ ,  $x_t = m_t^2/m_W^2$  ( $m_t$  and  $m_W$  are the masses of the top quark and  $W$  gauge boson, respectively),  $V_{ij}$  are the elements of the Cabibbo-Kabayashi-Maskawa (CKM) mixing matrix.  $f(z)$  and  $\kappa(z)$  ( $\bar{\eta} = \kappa(0)$ ) with  $z = m_c^{pole}/m_b^{pole}$  are the phase-space and quantum chromodynamics(QCD) correction factors for the decay  $B \rightarrow X_c e \bar{\nu}$  [5]. For  $z = 0.29$ , one finds  $f(z) = 0.54$  and  $\kappa(z) = 0.88$ . The function  $X(x_t)$  describes the top quark contribution and is given by [5]

$$X(x_t) = X_0(x_t) + \frac{\alpha_s}{4\pi} X_1(x_t) \quad (2)$$

with

$$X_0(x) = -\frac{x}{8} \left[ \frac{2+x}{1-x} + \frac{6-3x}{(1-x)^2} \ln[x] \right], \quad (3)$$

and the QCD correction  $X_1(x_t)$  can be found in [5]. As mentioned previously, the SM predictions for  $B \rightarrow X_{s,d} \nu \bar{\nu}$  are remarkably free from uncertainties. All the parameters entering in Eq.(1) are known with good accuracy. Since the decay  $B \rightarrow X_d \nu \bar{\nu}$  is further suppressed by the ratio  $|V_{td}/V_{ts}|^2 \sim 0.04$ , the decay  $B \rightarrow X_s \nu \bar{\nu}$  is more interesting experimentally. We here consider the decay  $B \rightarrow X_s \nu \bar{\nu}$  only. The experimental upper limit

$$\mathcal{B}(B \rightarrow X_s \nu \bar{\nu}) < 6.4 \times 10^{-4} \quad \text{at } 90\% C.L. \quad (4)$$

has been reported last year by ALEPH collaboration [6] at LEP, which is close to the SM prediction of  $(3.5 \pm 0.7) \times 10^{-5}$  [1]. The decay  $B \rightarrow X_s \nu \bar{\nu}$  may be accessible at B factories if background problems can be resolved. The decay  $B \rightarrow X_s \nu \bar{\nu}$  can probe many new physics scenarios and has been studied for example in the Technicolor models [7], the two-Higgs-doublet models (2HDM) of type-II and the supersymmetric models [8].

In this paper, we calculate the new physics contributions to the rare decay  $B \rightarrow X_s \nu \bar{\nu}$  due to the effective  $b\bar{s}Z$  coupling induced by the charged-Higgs penguin diagrams in the so-called model III: the 2HDM with flavor changing (FC) couplings [9]. In the 2HDM, the tree level flavor changing scalar currents are absent if one introduces an *ad hoc* discrete symmetry to constrain the 2HDM scalar potential and Yukawa Lagrangian. Lets consider a Yukawa Lagrangian of the form [9]

$$\mathcal{L}_Y = \eta_{ij}^U \bar{Q}_{i,L} \tilde{\phi}_1 U_{j,R} + \eta_{ij}^D \bar{Q}_{i,L} \phi_1 D_{j,R} + \xi_{ij}^U \bar{Q}_{i,L} \tilde{\phi}_2 U_{j,R} + \xi_{ij}^D \bar{Q}_{i,L} \phi_2 D_{j,R} + h.c., \quad (5)$$

where  $\phi_i$  ( $i = 1, 2$ ) are the two Higgs doublets,  $\tilde{\phi}_{1,2} = i\tau_2 \phi_{1,2}^*$ ,  $Q_{i,L}$  with  $i = (1, 2, 3)$  are the left-handed quarks,  $U_{j,R}$  and  $D_{j,R}$  are the right-handed up- and down-type quarks, while  $\eta_{i,j}^{U,D}$  and  $\xi_{i,j}^{U,D}$  ( $i, j = 1, 2, 3$  are family index) are generally the nondiagonal matrices of the Yukawa coupling. By imposing the discrete symmetry ( $\phi_1 \rightarrow -\phi_1, \phi_2 \rightarrow \phi_2, D_i \rightarrow -D_i, U_i \rightarrow \mp U_i$ ) one obtains the so called model I and II. One finds the model III if no discrete symmetry is imposed. In model III, there are also five physical Higgs bosons: the charged scalar  $H^\pm$ , the neutral CP even scalars  $H^0$  and  $h^0$  and the CP odd pseudoscalar  $A^0$ .

After the rotation that diagonalizes the mass matrix of the quark fields, the Yukawa Lagrangian of quarks are the form [9],

$$\mathcal{L}_Y^{III} = \eta_{ij}^U \bar{Q}_{i,L} \tilde{\phi}_1 U_{j,R} + \eta_{ij}^D \bar{Q}_{i,L} \phi_1 D_{j,R} + \hat{\xi}_{ij}^U \bar{Q}_{i,L} \tilde{\phi}_2 U_{j,R} + \hat{\xi}_{ij}^D \bar{Q}_{i,L} \phi_2 D_{j,R} + h.c., \quad (6)$$

where  $\eta_{ij}^{U,D} = m_i \delta_{ij} / v$  correspond to the diagonal mass matrices of quarks and  $v \approx 246 \text{ GeV}$  is the vacuum expectation value of  $\phi_1$ , while the neutral and charged FC couplings will be [9]

$$\hat{\xi}_{neutral}^{U,D} = \xi^{U,D}, \quad \hat{\xi}_{charged}^U = \xi^U V, \quad \hat{\xi}_{charged}^D = V \xi^D, \quad (7)$$

where  $V_{CKM}$  is the Cabibbo-Kabayashi-Maskawa mixing matrix, and

$$\xi_{ij}^{U,D} = \frac{\sqrt{m_i m_j}}{v} \lambda_{ij}. \quad (8)$$

where the coupling parameters  $\lambda_{ij}$  ( $i, j = (1, 2, 3)$  are the generation index) are free parameters to be determined by experiments. As pointed in Ref. [9], the data of  $K^0 - \bar{K}^0$  and  $B_d^0 - \bar{B}_d^0$  mixing processes put severe constraint on the FC couplings involving the first two generations of quarks. One therefore assume that:

$$\lambda_{ij} = 0, \quad \text{for } i = 1, 2, \quad \text{and } j = 1, 2, 3. \quad (9)$$

From the CERN  $e^+e^-$  collider (LEP) and Tevatron searches for charged Higgs bosons [10], the combined constraint in the  $(m_{H^+}, \tan \beta)$  plane has been given in Ref. [11]: the direct lower limit is  $m_{H^+} > 77 \text{ GeV}$ . In this paper, we consider Chao, Cheung and Keung (CCK) scenario of the model III [12]: only the couplings  $\lambda_{tt}$  and  $\lambda_{bb}$  are non-zero. In this scenario, the existence of a charged Higgs boson with  $m_{H^+} \sim 200 \text{ GeV}$  is still allowed [12,13,14].

From the CLEO data of  $\mathcal{B}(B \rightarrow X_s \gamma)$ , some constraint on  $m_{H^+}$  in model III can also be derived [12]. New precision measurements of  $B \rightarrow X_s \gamma$  are reported recently by CLEO [15] and by Belle Collaboration [16]. Combining with previous determinations [11], the world average as given in Ref. [17] reads:  $\mathcal{B}(B \rightarrow X_s \gamma)^{exp} = (3.23 \pm 0.42) \times 10^{-4}$ . At the  $2\sigma$  level, we have  $2.4 \times 10^{-4} \leq \mathcal{B}(B \rightarrow X_s \gamma) \leq 4.1 \times 10^{-4}$ . Fig.1 is the contour plot of the branching ratio  $\mathcal{B}(B \rightarrow X_s \gamma)$  versus  $|\lambda_{tt}|$  and  $|\lambda_{bb}|$  for  $m_{H^+} = 200 \text{ GeV}$  and  $\theta = \theta_{tt} - \theta_{bb} = 0^\circ$ . It is easy to see that most part of the parameter space of  $|\lambda_{tt}|$  and  $|\lambda_{bb}|$  has been excluded, only the narrow regions between two dots curves and two solid curves are still allowed by the data of  $B \rightarrow X_s \gamma$ . In the region of  $\lambda_{tt} \geq 5$ , the upper (lower) band has a weak (moderate)

dependence on the value of  $\lambda_{bb}$ :  $\lambda_{bb} = 2.7 \pm 0.2$  for the upper band and  $\lambda_{bb} = 1.0_{-0.4}^{+0.6}$  for the lower band.

Under the assumption of neglecting all non- $Z$ -mediated contributions, Buchalla et al. [18] studied the constraints on the effective couplings  $Z_{bs}^{L,R}$  obtained by comparing the theoretical predictions of the branching ratios of  $B \rightarrow X_s \nu \bar{\nu}$ ,  $X_s l^+ l^-$  and  $B \rightarrow K^* \mu^+ \mu^-$  decay modes with the experimental measurements [6,19,20]<sup>1</sup>:

$$\sqrt{|Z_{bs}^L|^2 + |Z_{bs}^R|^2} \lesssim 0.22, \quad \text{from } \mathcal{B}(B \rightarrow X_s \nu \bar{\nu}) < 6.4 \times 10^{-4}, \quad (10)$$

$$\sqrt{|Z_{bs}^L|^2 + |Z_{bs}^R|^2} \lesssim 0.15, \quad \text{from } \mathcal{B}(B \rightarrow X_s l^+ l^-) < 4.2 \times 10^{-5}, \quad (11)$$

$$|Z_{bs}^{L,R}| \lesssim 0.13, \quad \text{from } \mathcal{B}(B \rightarrow K^* \mu^+ \mu^-)^{n.r.} < 4.0 \times 10^{-6} \quad (12)$$

Among the three modes,  $B \rightarrow X_s \nu \bar{\nu}$  decay is the cleanest mode. Since the SM contributions are  $Z_{bs}^L = V_{tb}^* V_{ts} C_0(x_t) \sim 0.04$  and  $Z_{bs}^R = 0$ , a new physics enhancement to the branching ratio  $\mathcal{B}(B \rightarrow X_s \nu \bar{\nu})$  as large as a factor of  $(0.22/0.04)^2 \sim 30$  is still allowed by the first bound. The third bound is stronger but subject to large theoretical uncertainties in the form factors and the assumptions on the non-perturbative non-resonant contributions, and therefore less reliable. The detailed discussions for the new physics enhancement to  $\mathcal{B}(B \rightarrow X_s \nu \bar{\nu})$  and the possible constraints on the FC couplings of model III will be given below.

For the decay processes considered here, as illustrated in Fig.2, the new  $Z$ -penguin diagrams with internal top quarks obtained by replacing the  $W$  gauge boson with the charged-Higgs boson dominate the new physics corrections. The charged-Higgs box diagram does not contribute because the Yukawa coupling  $H^+ l \nu$  is zero. The neutral Higgs bosons also do not contribute at tree level or one-loop level in the CCK scenario of model III [14]. In the calculation, we will use dimensional regularization to regulate all the ultraviolet divergences in the virtual loop corrections and adopt the modified minimal subtracted ( $\overline{MS}$ ) renormalization scheme.

By analytical evaluations of the Feynman diagrams, we find the effective  $b\bar{s}Z$  vertex induced by the charged-Higgs exchanges,

$$\Gamma_{Z\mu} = \frac{1}{16\pi^2} \frac{g^3}{\cos\theta_W} V_{ts}^* V_{tb} \bar{s}_L \gamma_\mu b_L C_0^N(y_t) \quad (13)$$

with

$$\begin{aligned} C_0^N(y_t) = & -\frac{x_t}{16} \left\{ \left[ \frac{y_t}{1-y_t} + \frac{y_t}{(1-y_t)^2} \ln[y_t] \right] |\lambda_{tt}|^2 \right. \\ & + \frac{4m_b^2 \sin^2\theta_W}{3m_t^2} \left[ \frac{3y_t - y_t^2}{4(1-y_t)^2} + \frac{y_t}{(1-y_t)^3} \ln[y_t] \right] |\lambda_{tt}|^2 \\ & + \frac{m_b^2}{m_t^2} \left[ \frac{3y_t - y_t^2}{4(1-y_t)^2} + \frac{y_t}{(1-y_t)^3} \ln[y_t] \right. \\ & \left. \left. + \left(1 - \frac{4}{3} \sin^2\theta_W\right) \left( \frac{y_t}{1-y_t} + \frac{y_t}{(1-y_t)^2} \ln[y_t] \right) \right] |\lambda_{tt}\lambda_{bb}| e^{i\theta} \right\} \quad (14) \end{aligned}$$

---

<sup>1</sup>For  $B \rightarrow X_s \nu \bar{\nu}$  decay, we here use the new ALEPH measurement [6]  $\mathcal{B}(B \rightarrow X_s \nu \bar{\nu}) < 6.4 \times 10^{-4}$  instead of the old one as used in Ref. [18].

where  $y_t = m_t^2/m_{H^+}^2$ ,  $\theta_W$  is the Weinberg angle, and  $\theta = \theta_{tt} - \theta_{bb}$ . It is easy to see that the value of  $C_0^N$  ( i.e, the size of new physics corrections) is controlled by the first term of Eq.(14). The second and third terms of Eq.(14) are strongly suppressed by the factor of  $m_b^2/m_t^2 \approx 8 \times 10^{-4}$ . In other words, the parameter  $\lambda_{tt}$  dominates the new physics contribution, while  $\lambda_{bb}$  and  $\theta$  play a minor role only. When the new physics contributions are taken into account, the  $X$  function in Eqs.(2) takes the form

$$X(x_t, y_t) = X(x_t) + C_0^N(y_t), \quad (15)$$

where function  $X(x_t)$  has been given in Eq.(2).

In the numerical calculations, the following parameters will be used as the standard input:  $M_W = 80.42\text{GeV}$ ,  $\alpha_{em} = 1/129$ ,  $\sin^2 \theta_W = 0.23$ ,  $m_c = 1.5 \text{ GeV}$ ,  $m_b = 4.88 \text{ GeV}$ ,  $m_t \equiv \overline{m}_t(m_t) = 168 \pm 5 \text{ GeV}$ ,  $\Lambda_{MS}^{(5)} = 0.225\text{GeV}$ ,  $\mathcal{B}(B \rightarrow X_c e \bar{\nu}) = 10.4 \pm 0.6\%$ ,  $A = 0.847$ ,  $\lambda = 0.2205$ ,  $R_b = 0.38 \pm 0.08$ ,  $\gamma = (60 \pm 20)^\circ$  and  $\theta = 0^\circ - 30^\circ$ . For the definitions and values of these input parameters, one can see Refs. [1,11]. We have neglected the small errors of those well measured quantities, but keep the errors for remaining parameters in order to estimate the uncertainties of the theoretical predictions. We treat the masses of charged-Higgs boson as semi-free parameters  $m_{H^+} = 200 \pm 100 \text{ GeV}$ .

Fig.3 shows the  $\lambda_{tt}$  dependence of the branching ratio  $\mathcal{B}(B \rightarrow X_s \nu \bar{\nu})$  in the SM and model III for  $\lambda_{bb} = 2.7$ ,  $\theta = 0^\circ$ , and  $m_{H^+} = 150$  (short-dashed curve), 200 (solid curve) and 250 GeV (dot-dashed curve), respectively. The dotted line in Fig.3 is the SM prediction:  $\mathcal{B}(B \rightarrow X_s \nu \bar{\nu}) = 3.5 \times 10^{-5}$ . The upper solid line corresponds to the ALEPH upper limit:  $\mathcal{B}(B \rightarrow X_s \nu \bar{\nu}) < 6.4 \times 10^{-4}$ . The new physics contribution in model III can provide one to two orders of enhancement to the branching ratio  $\mathcal{B}(B \rightarrow X_s \nu \bar{\nu})$ . Furthermore, the constraint on  $\lambda_{tt}$  can be read off directly from Fig.3:  $\lambda_{tt} \leq 6.4$  for  $m_{H^+} \approx 200 \text{ GeV}$ , which is complementary to the limits obtained from the  $B \rightarrow X_s \gamma$  data.

In order to reduce the effects of uncertainties of input parameters, we can denote the model III prediction normalized to the SM results by  $R$ ,

$$R(B \rightarrow X_s \nu \bar{\nu}) = \frac{\mathcal{B}(B \rightarrow X_s \nu \bar{\nu})^{III}}{\mathcal{B}(B \rightarrow X_s \nu \bar{\nu})^{SM}} = \frac{|X(x_t, y_t)|^2}{|X(x_t)|^2} \quad (16)$$

The uncertainties of most input parameters are clearly cancelled out in such ratio.

In Fig.4, we show the dependence of the ratio  $R$  on the mass  $m_{H^+}$  by using the input parameters as specified before and setting two representative sets of Yukawa couplings allowed by the CLEO data of  $B \rightarrow X_s \gamma$ : Set-A:  $(\lambda_{tt}, \lambda_{bb}) = (6, 2.7)$ (solid curve); and Set-B:  $(\lambda_{tt}, \lambda_{bb}) = (3, 0.5)$ (short-dashed curve). The dotted line in Fig.4 corresponds to the ALEPH upper limit  $R(B \rightarrow X_s \nu \bar{\nu})^{exp} < 18.3$ . The ratio  $R$  has a very weak dependence on both the ratio  $m_t/m_W$  and the angle  $\theta$  for  $m_t(m_t) = 168 \pm 5 \text{ GeV}$  and  $\theta = 0^\circ - 30^\circ$ .

Although the experimental upper bound on  $\mathcal{B}(B \rightarrow X_s \nu \bar{\nu})$  is still a factor of 18 above the SM expectation, this upper bound has lead to interesting constraints on the parameter space of model III. The  $B \rightarrow X_s \nu \bar{\nu}$  decay can probe many new physics scenarios [3], and deserve the maximum of attention. We know that the measurement of  $B \rightarrow X_s \nu \bar{\nu}$  decay is experimentally very challenging, the gap between SM expectation and experimental limits could decrease in the next few years at B-factory experiments. The observation of these decays in the near future will enable us to confirm or exclude the new physics contributions,

or at least put some stringent constraints on two-Higgs doublet models and other new physics models.

In summary, we calculated the new physics contribution to theoretically very clean rare decay  $B \rightarrow X_s \nu \bar{\nu}$  in the third type of two-Higgs-doublet models. Within the considered parameter space, we found that: (a) the new physics contribution can provide one to two orders of enhancements to the rare decays  $B \rightarrow X_s \nu \bar{\nu}$  and can saturate the experimental bound on  $\mathcal{B}(B \rightarrow X_s \nu \bar{\nu})$  in some regions of the parameter space; (b) besides the CLEO data of  $B \rightarrow X_s \gamma$ , the ALEPH upper limit on  $\mathcal{B}(B \rightarrow X_s \nu \bar{\nu})$  also lead to further constraint on the size of  $\lambda_{tt}$ :  $\lambda_{tt} < 6.4$  for  $\lambda_{bb} = 2.7$  and  $m_{H^+} = 200$  GeV.

### ACKNOWLEDGMENTS

Xiao Zhenjun acknowledges the support by the National Natural Science Foundation of China under Grant No.10075013, and by the Research Foundation of Nanjing Normal University under Grant No.214080A916.

## REFERENCES

- [1] A.J. Buras, in *Flavour Physics: CP violation and rare Decays*, Lectures given at International School of Subnuclear Physics, Erice, Italy, 2000, hep-ph/0101336.
- [2] X.G.He, T.D. Nguyen, and R.R. Volkas, Phys.Rev. **D38**(1988)814; W.Sikba and J.Kalinowski, Nucl.Phys. **B404**, (1993)3.
- [3] Y.Grossman, Z.ligeti and E.Nardi, Nucl.Phys. **B465** (1996)369.
- [4] Y.B.Dai, C.S.Huang and H.W.Huang, Phys.Lett. **B390** (1997)257; K.S.Babu, C.Kolda, Phys.Rev.Lett. **84** (2000)228; C.S.Huang, W.Liao, Q.S.an, and S.H.Zhu, Phys.Rev. **D63** (2001)114021; C.S.Huang and W. Liao, Phys.Lett. **B525** (2002)107.
- [5] G.Buchalla, A.J.Buras and M.E. Lautenbacher, Rev.Mod.Phys. **68** (1996)1125.
- [6] R.Barate *et al.*, ALEPH Collab., Eur.Phys.J. **C19** (2001)213.
- [7] Z.J.Xiao, L.X.Lü, H.K.Guo and G.R.Lu, Chin.Phys.Lett. **16** (1999)88; Z.J.Xiao, L.Q.Jia, L.X.Lü and G.R.Lu, Communi.Theor.Phys. **33** (2000)269.
- [8] A.J.Buras, P.Gambino, M.Gorbahn, S.Jäger and L. Silvestrini, Nucl.Phys. **B592** (2001)55; C.Boeth, A.Buras, F.Krüger and J.Urban, Nucl.Phys. **B630**(2002)87.
- [9] D.Atwood, L.Reina and A.Soni, Phy.Rev. **D55** (1997)3156, and reference therein.
- [10] L3 Collaboration, M.Acciarri *et al.*, Phys.Lett. **B466** (1999)71; D0 Collaboration, B.Abbott *et al.*, Phys.Rev.Lett. **82**, (1999)4975; CDF Collaboration, T.Affolder *et al.*, Phys.Rev. **D62** (2000)012004.
- [11] Particle Data Group, D.E.Groom *et al.*, Eur.Phys.J. **C15** (2000)1.
- [12] D. B. Chao, K. Cheung and W.Y. Keung, Phys.Rev. **D59** (1999)115006.
- [13] Z.J.Xiao, C.S.Li and K.T. Chao, Phys.Rev. **D62** (2000)094008; Phys.Lett. **B473** (2000) 148.
- [14] Z.J.Xiao, C.S.Li and K.T. Chao, Phys.Rev. **D63** (2001)074005.
- [15] CLEO Collaboration, S. Chen, *et al.*, Phys.Rev.Lett. **87** (2001)251807.
- [16] Belle Collaboration, K.Abe, *et al.*, Phys.Lett. **B511** (2001)151.
- [17] G.Isidori, Lepton Photon 2001, Rome, Italy, July 2001; hep-ph/0110255.
- [18] G. Buchalla, G.Hiller and G.Isidori, Phys.Rev. **D63**(2001)014015.
- [19] The CLEO Collaboration, S. Glenn *et al.*, Phys.Rev. Lett. **80**(1998)2289.
- [20] CDF Collaboration, T. Affolder *et al.*, Phys.Rev. Lett. **83**(1999)3378.

FIGURES

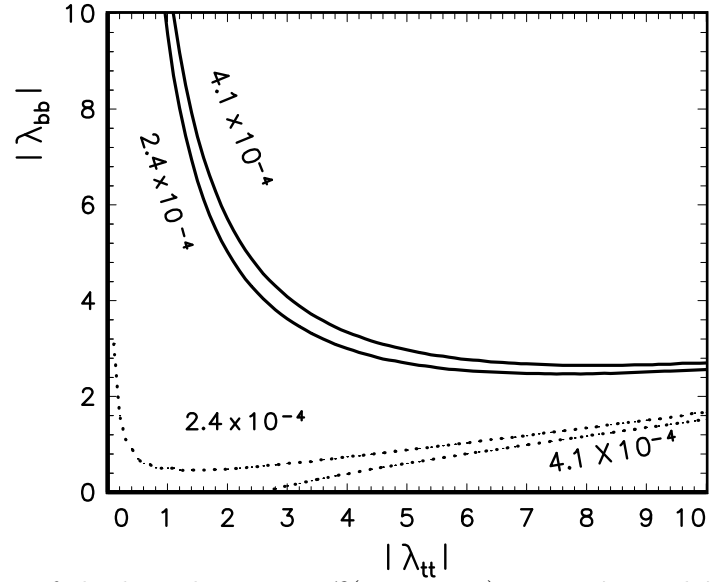


FIG. 1. Contour plot of the branching ratio  $\mathcal{B}(B \rightarrow X_s \gamma)$  versus  $\lambda_{tt}$  and  $\lambda_{bb}$  for  $m_{H^+} = 200$  GeV and  $\theta = 0^\circ$ . The narrow regions between two dotted curves and two solid curves are still allowed by the data:  $2.4 \times 10^{-4} \leq \mathcal{B}(B \rightarrow X_s \gamma) \leq 4.1 \times 10^{-4}$ .



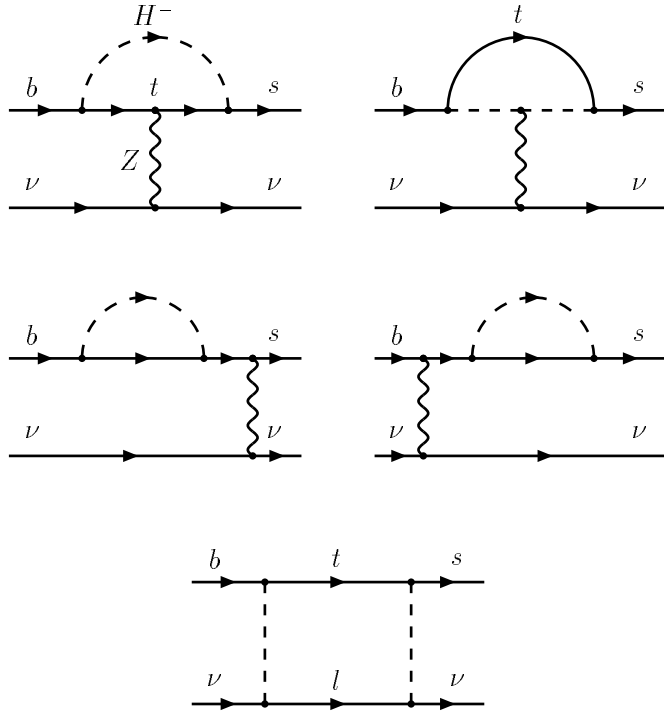


FIG. 2. The typical new  $Z^0$ -penguin, self-energy and box diagrams for  $B \rightarrow X_s \nu \bar{\nu}$  decay in model III.

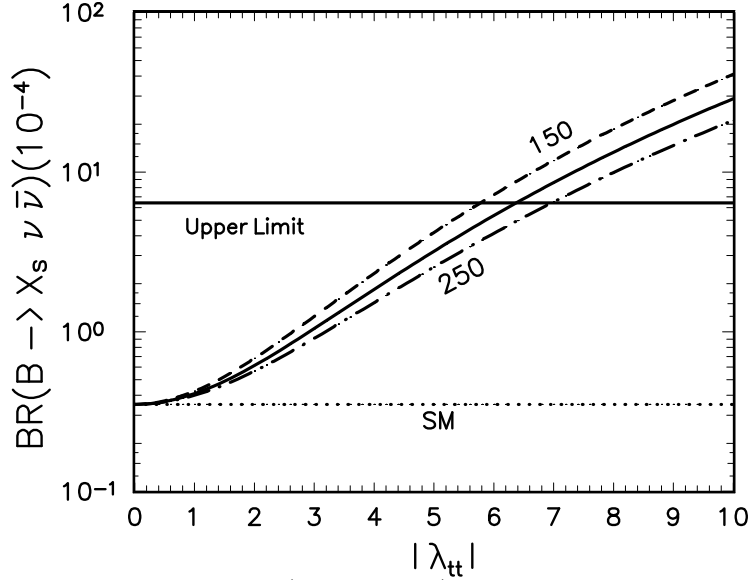


FIG. 3. Plots of the branching ratio  $\mathcal{B}(B \rightarrow X_s \nu \bar{\nu})$  versus  $\lambda_{tt}$  in the SM and model III for  $\lambda_{bb} = 2.7$ , and  $m_{H^+} = 150$  (short-dashed curve), 200 (solid curve) and 250 GeV (dot-dashed curve), respectively. The dotted line is the SM prediction, while the upper solid line corresponds to the ALEPH upper limit:  $\mathcal{B}(B \rightarrow X_s \nu \bar{\nu}) < 6.4 \times 10^{-4}$ .

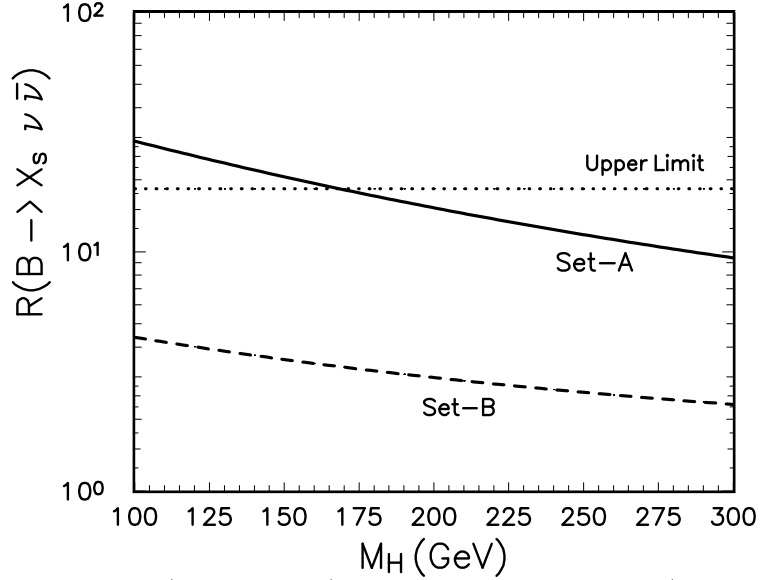


FIG. 4. Plots of the ratio  $R(B \rightarrow X_s \nu \bar{\nu})$  versus  $m_{H^+}$  for Set-A (solid curve) and Set-B (short-dashed curve) Yukawa couplings in model III. The dotted line refers to the ALEPH upper limit:  $\mathcal{B}(B \rightarrow X_s \nu \bar{\nu}) < 6.4 \times 10^{-4}$ .